Research Journal of Chemical Sciences ISSN 2231-606X
Vol. **4(4),** 71-77, April **(2014)** *Res. J. Chem. Sci.*

The Phase Evolution at High-Temperature Treatment of the Oxide-Fluoride Ceramic Flux

Sokolsky V.E.[1*], Roik O.S.[1], Davidenko A.O.[1], Kazimirov V.P.[1], Lisnyak V.V.[1], Galinich V.I.[2] and Goncharov I.A.[2]
[1]Chemical Department, Kyiv National Taras Shevchenko University, 01601 Kyiv, UKRAINE
[2]The E.O. Paton Electric Welding Institute of NAS of Ukraine, 03680 Kyiv, UKRAINE

Available online at: www.isca.in, www.isca.me
Received 7th March 2014, revised 1st April 2014, accepted 15th April 2014

Abstract

The products of high temperature treatment of the oxide-fluoride ceramic flux of the composition MgO (30.0 mass. %) – Al_2O_3 (25.0 mass. %) – SiO_2 (20.0 mass. %) – CaF_2 (25.0 mass. %), which was obtained using liquid glass as a binder, were examined by means of X-ray powder diffraction (XRPD). The slag obtained by the ceramic flux remelting at 1773 K according to XRPD data contains $MgAl_2O_4$, CaF_2 and Mg_2SiO_4 phases. High temperature X-ray diffraction data (HTXRD), collected at heating regime, show that the initial components exist in the ceramic flux at temperatures (T) ≤ 1473 K. The partial melting of the ceramic flux is accompanied with formation of crystalline $MgAl_2O_4$ phase. Detail examination of the slag samples by means of scanning electron microscopy (SEM) and energy dispersive X-ray (EDX) microanalysis confirms results of the XRPD and HTXRD studies.

Keywords: X-ray diffraction (XRD), ceramic flux, energy dispersive X-ray (EDX) microanalysis, spinel, high temperature X-ray diffraction (HTXRD), slag, scanning electron microscopy (SEM).

Introduction

Electroslag surfacing (ESS)[1–3] are used worldwide for restoration of steel components by deposition of protective layer of corrosion resistant materials. The ESS under protective layer of fused ceramic fluxes is one of the known techniques applied for the surfacing of metal at metalwork production[4,5]. The high-temperature reactions of the ceramic flux components can affect on the quality of ESS that is why, it is desirable to know peculiarities of high-temperature chemical interaction of the ceramic fluxes components and the crystallization behavior of resulted slags to be used for a design of advanced fluxes.

The solidification, crystallization behavior and phase formation were intensively examined for mixed oxide slags[6–8]. However, these issues for the oxide-fluoride fluxes, including that adopted in the ESS, and their slags have not received much attention by researchers. Only the solidification structures of CaO–SiO_2-rich quaternary CaO–SiO_2–Al_2O_3–MgO) and quinary CaO–SiO_2–MgO–Al_2O_3 (–5 wt. % CaF_2) liquid slags containing at least 10 wt. % MgO and up to 30 wt. % Al_2O_3 were reported in the literature[9,10]. However, to the best of our knowledge no such information available for (CaO-free MgO-rich) oxide-fluoride ceramic fluxes with high (up to 25 mass. %) CaF_2 content, which are frequently used for the ESS[5].

Earlier we reported on the transformation of crystalline phases of the SiO_2-rich oxide-fluoride ceramic flux at heating[11]; the present paper is devoted to examination of the MgO-rich ceramic flux.

Material and Methods

Ceramic flux and slags preparation: The MgO-rich oxide-fluoride ceramic flux was prepared in three steps: i. Calcined reagents of MgO, Al_2O_3, SiO_2 and CaF_2 taken in appropriate ratio (30 mass. % MgO – 25 mass. % Al_2O_3 – 20 mass. % SiO_2 – 25 mass. % CaF_2) were mixed; ii. the powders mixture was bound with liquid glass (sodium/potassium silicates solution); iii. the wet product was granulated and annealed at 873 K.

The ceramic flux samples were incrementally heated to 1773 K in Mo crucibles by induction heating. The flux samples were remelted and slags were obtained. These slags were quenched and the samples taken from the upper and the inner parts of the crucible were subjected to the further examination.

Ceramic flux and slags characterization: The ceramic flux and the slag samples were subjected to X-rays fluorescence (XRF) and X-ray powder diffraction (XRPD). The ceramic flux evolution at heating was examined by means of high-temperature X-ray diffraction (HTXRD). The slags samples obtained from the ceramic flux were studied by using scanning electron microscopy (SEM).

XRF analysis: The composition of granulated and annealed samples of the ceramic flux was determined with a Philips X' Unique II (model 1480, Rh X-ray tube) XRF spectrometer.

XRPD analysis: XRPD patterns were collected at 298 K by using a DRON-3M diffractometer (Fe-filtered CuKα-radiation, λ = 1.5406 Å). The experimental XRPD patterns were refined,

indexed and simulated by means of programs of the PowderCell2.4[12]. The quantitative X-ray diffraction phase (QXRPD) analysis was performed using the Match software[13].

HTXRD analysis: was used to study the phase formation at heating of the ceramic flux. The intensity X-ray patterns were recorded at temperatures of 873 K, 1073 K, 1273 K, 1473 K, 1573 K, 1673 K and 1773 K using a high-temperature θ–θ diffractometer operated with MoKα radiation (λ = 0.7107 Å). The apparatus, measurement and calculation routines were reported earlier[11, 14].

SEM analysis: The slags obtained by the ceramic flux remelting at 1773 K and subsequent quenching were examined by SEM with Jeol JSM 7700 F microscope. The energy dispersive X-ray (EDX) microanalysis was performed with an Oxford Inca spectrometer that attached to the JSM 7700 F microscope. To prevent charges caused by the electron beam in the low conductive solids, 3 nm thick layer of pure platinum was sputtered on the surface of the samples.

Results and Discussion

The initial components composition used for the preparation of the ceramic flux and the resulted average composition found from the XRF data for the final granulated and annealed product, were listed in table-1.

Figure-1 depicts theoretical intensity curve and the XRPD pattern collected for the granulated and annealed sample. The theoretical intensity curve was simulated and refined for the mixture of components, which are presented in the composition of the ceramic flux. The refinement is based on the reflections of α-quartz (SiO_2), corundum (trigonal Al_2O_3), periclase (cubic MgO) and fluorite (CaF_2) phases. According to the XRPD data, only the initial components and no other crystalline phases were found in the ceramic flux.

Figure-2 shows XRPD and HTXRD patterns recorded for the sample of granulated and annealed ceramic flux over the temperature range of 298 K to 1773 K. According to the figure-2, the crystalline phases of the main components remain in the ceramic flux at $T \leq 1473$ K. The liquid phase was formed at the temperature c.a. 1473 K due to melting of the sinter of the liquid glass with the major components of the flux. The figure-2 shows reduction of the intensity of observed diffraction peaks with heating. This reduction is caused by melting of the ceramic flux components. The partial melting of the ceramic flux at 1573 K is accompanied with formation of a new crystalline phase, which reflections were clearly seen on the figure-2, see HTXRD patterns from 6 to 8. Theoretical reflections of the $MgAl_2O_4$ spinel coincide well with the reflections registered experimentally at the temperatures above 1473 K. The complete melting of the flux is not observed below $T_m(MgAl_2O_4)$ = 2408 K. The HTXRD study indicates a complex nature of the interaction of the ceramic flux components before the formation of the slag.

Figure-3 shows experimental XRPD pattern of the slag that is obtained by the ceramic flux re-melting at 1773 K. The XRPD pattern is simulated and refined accounting reflections of the $MgAl_2O_4$, CaF_2 and Mg_2SiO_4 phases that are found by preliminary QXRPD analysis. The cubic spinel $MgAl_2O_4$ (space group $Fd\ \bar{3}m$, a = 0.8100 nm), cubic fluorite CaF_2 (space group $Fm\ \bar{3}m$, a = 0.546 nm), and orthorhombic forsterite Mg_2SiO_4 (space group $Pbnm$, a = 0.4822 nm, b = 1.1108 nm, c = 0.6382 nm) are the main crystalline phases in the slag.

SEM microphotos of the slag samples taken from the upper and from the inner parts of the crucible were shown on figure-4a-4d. Mg_2SiO_4, $MgAl_2O_4$ and CaF_2 phases were identified according to the SEM/EDX microanalysis data. The octahedral crystallites of spinel $MgAl_2O_4$, dendrites of CaF_2 about a hundred micrometers in size and also bulky phase of Mg_2SiO_4 are clearly seen from the figure-4d.

It is clearly seen from the figure-4a that in a continuous matrix of a one phase (the bright phase) are present the inclusion of another more dispersed phase (the dark phase) which was identified as Mg_2SiO_4. This conclusion is based on the EDX microanalysis data that collected from the regions limited in the figure-4a by rectangles and indicated as Spectrum 2 and 4. A zoom of the area highlighted in a black box on the figure-4a is shown on the figure-4b. The bright phase of very low crystallinity (amorphous-like phase), which is formed probably at melting of fusible components of the ceramic flux, can not be identified as a single compound by EDX. The similar assignment is true for the regions in the figure-4c indicated as spectrum 1 and 4 and corresponding to the partially crystallized low-melting phase.

Table-1
Composition of the ceramic flux

Composition	Components (mass. %)						
	MgO	**Al_2O_3**	**SiO_2**	**CaF_2**	**Na_2O**	**K_2O**	**Fe_2O_3**
Initial	30	25	20	25	-	-	-
Resulted	25.8	18.7	28.4	22.2	1.6	0.8	1.8

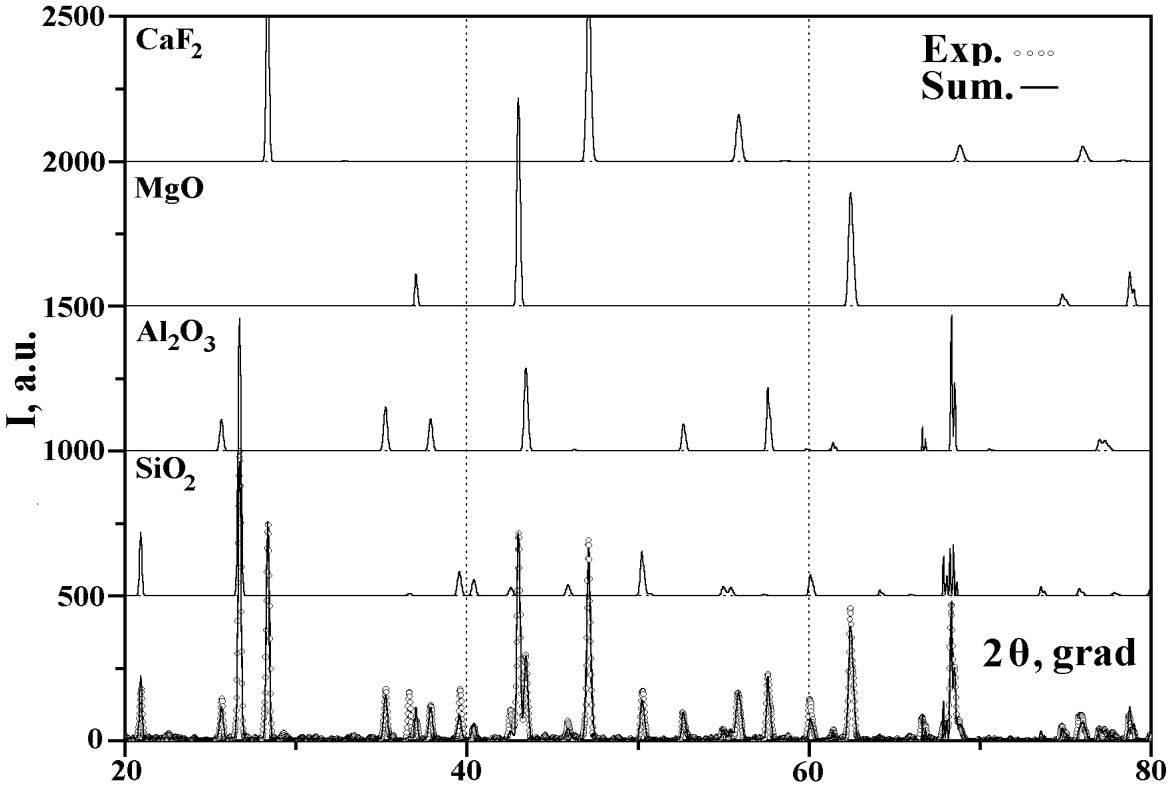

Figure-1
Experimental XRPD pattern (Exp.) and theoretical intensity curve (Sum.)

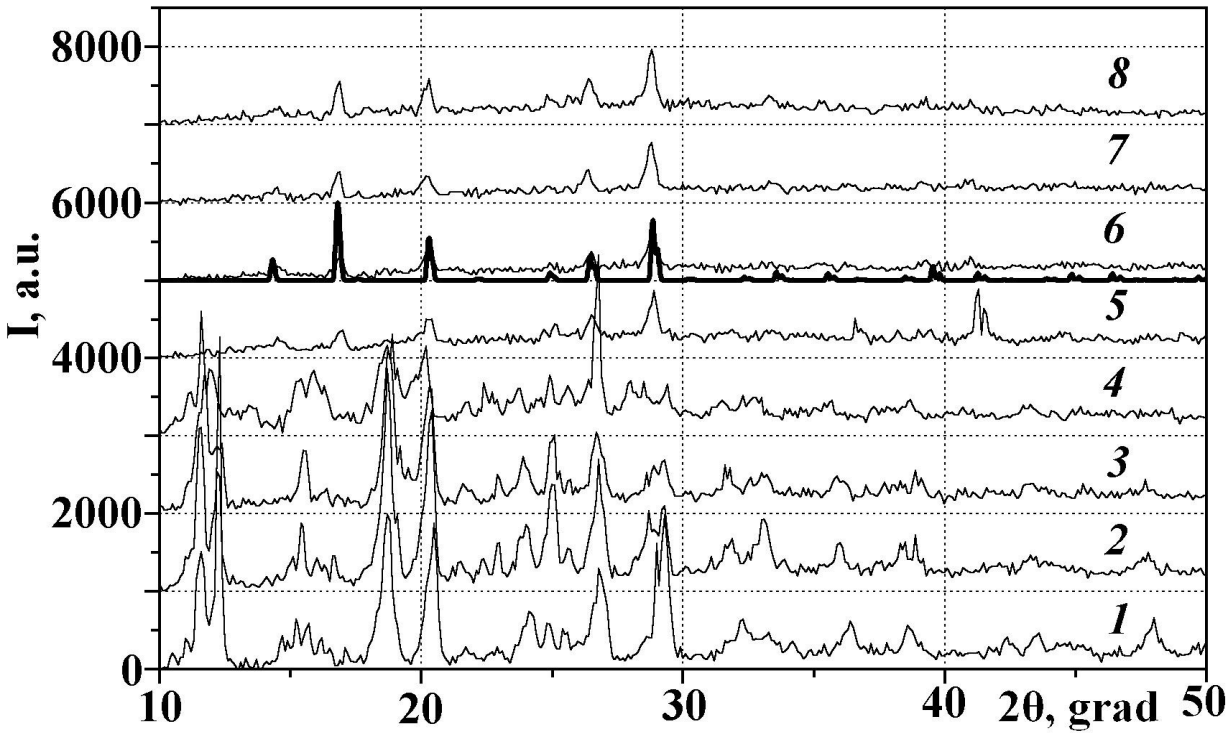

Figure-2
XRPD pattern at 298 K (1) and HTXRD patterns at 873 K (2), 1073 K (3), 1273 K (4), 1473 K (5), 1573 K (6), 1673 K (7) and 1773 K (8). HTXRD pattern (6) is combined with the pure $MgAl_2O_4$ spinel XRPD pattern (line)

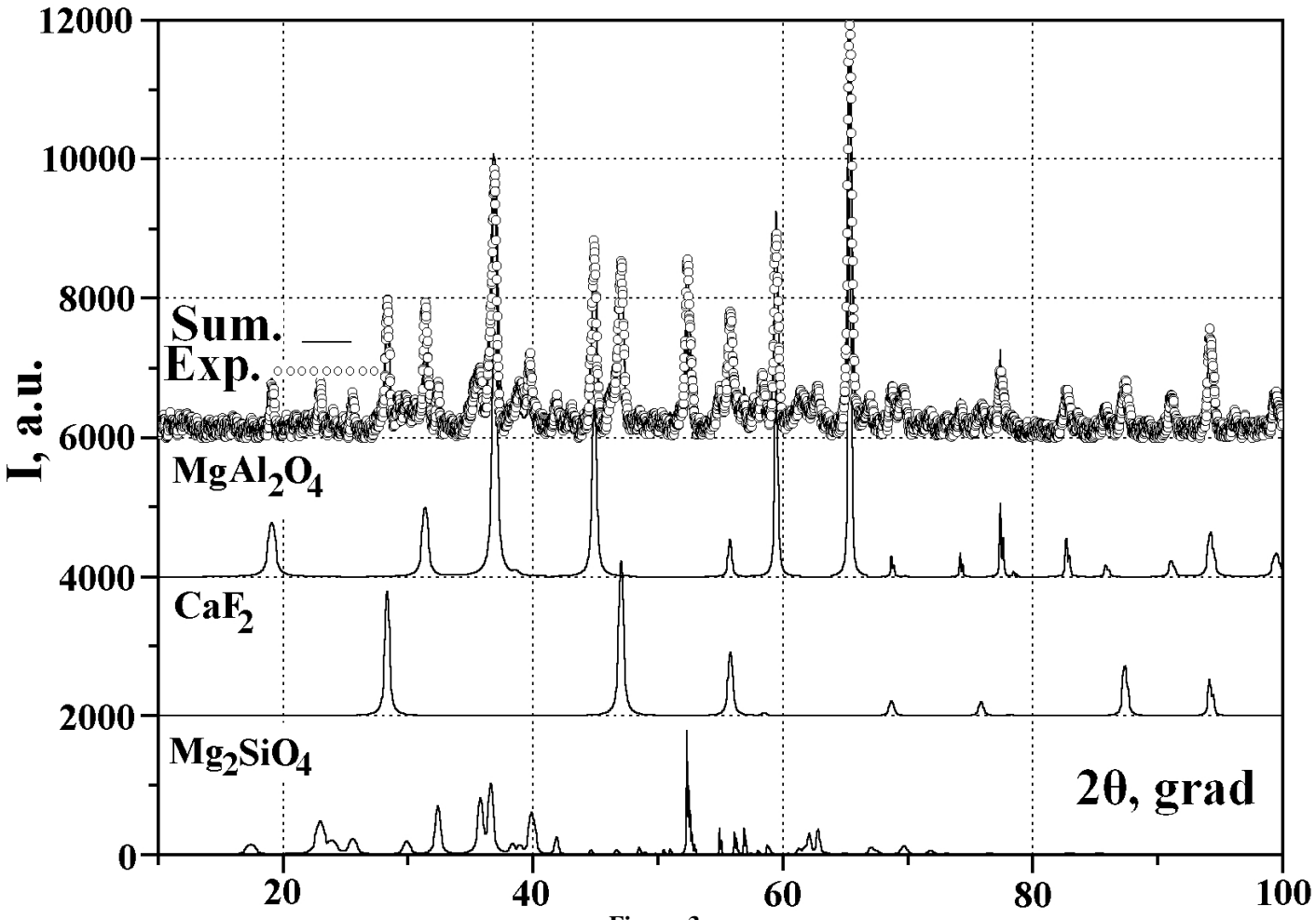

Figure-3
XRPD pattern of the slag

It should be noted that the EDX microanalysis data registered for the same phases in the samples taken from inner and upper parts of the crucible are differ from each other. The lowest content of impurities was registered by EDX in the $MgAl_2O_4$ and Mg_2SiO_4. The microanalysis data obtained for the region indicated as Spectrum 2 in the figure-4c can be interpreted as $Ca_xMg_{2-x}SiO_4$ solid solution, which contains an admixture of Al^{3+}. The presence of $Ca_xMg_{2-x}SiO_4$ solid solution in the slag could be explained as follows. Apparently, some of the calcium fluoride reacts with MgO and SiO_2 caused formation of $Ca_xMg_{2-x}SiO_4$. The composition of the region indicated by rectangle as Spectrum 3 in the figure-4c is closest to the stoichiometry of CaF_2. It was found from EDX data for the region indicated as Spectrum 5 in the figure-4c that sodium is concentrated mainly at the grain boundaries of crystallites as inclusions (up to 1.3 % at.) and no Na-rich fields or phases are found by the EDX analysis for the sample taken from the inner part of the crucible. It should be noted that the sample taken from the upper part of the crucible is saturated with the spinel $MgAl_2O_4$ phase.

In general the SEM/EDX microanalysis results are in a good agreement with the PXRD and HTXRD data obtained. SEM/EDX studies performed on the samples taken from the upper part of the crucible indicate on a more complex nature of interactions between the components than that realized in its inner part.

Since the upper parts of the crucible is saturated with spinel (SEM/EDX and HTXRD data), as compared with the inner parts, so one can assume that the spinel crystallites are lighter than the liquid phase and can float up to the melt surface. Thus, if the thermal expansion coefficient of the spinel and of the products of the liquid phase solidification are differ at the room temperature, consequently, the micro-stresses within the matrix of the solidified liquid phase should be realize. The latter results in a good separation of the slag crust from the ESS metal. High melting point and chemical resistance to various chemicals[15], e.g. surfacing slag components, is characteristic for $MgAl_2O_4$. So, these characteristics of $MgAl_2O_4$ can attract interest to the spinel as a component at the development of advanced ESS fluxes.

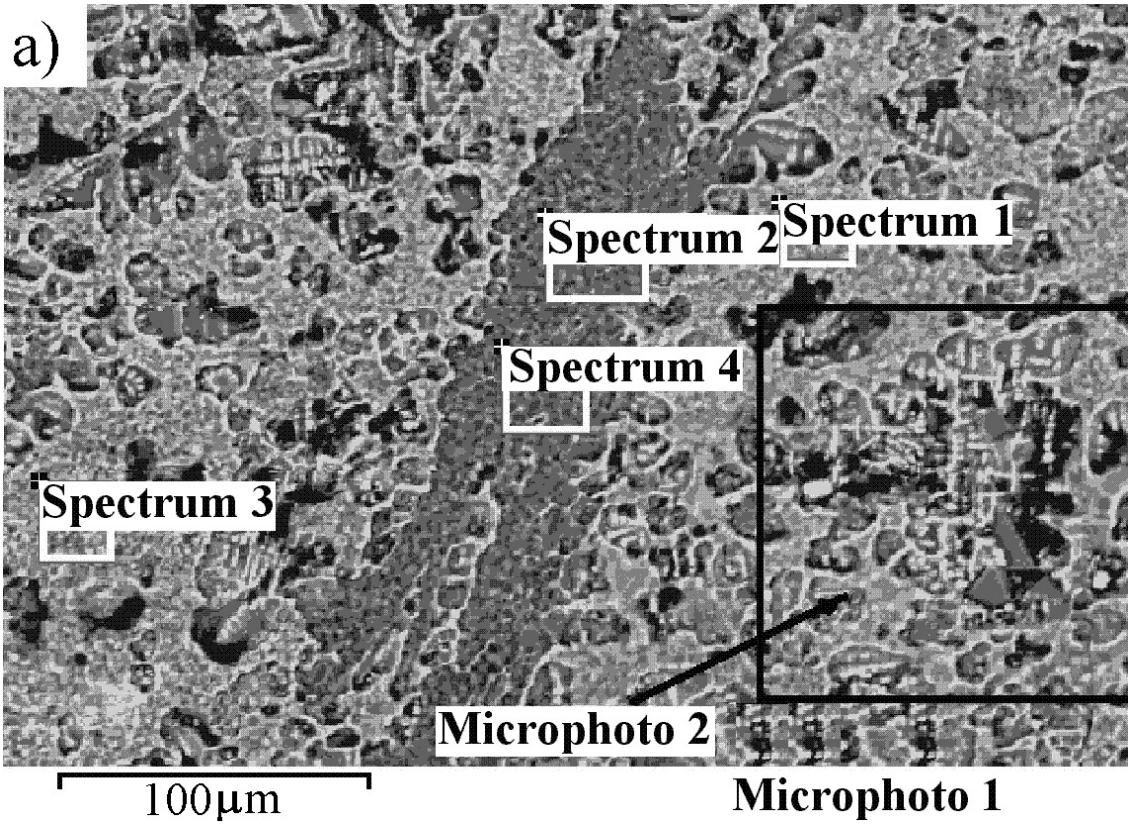

Figure-4A

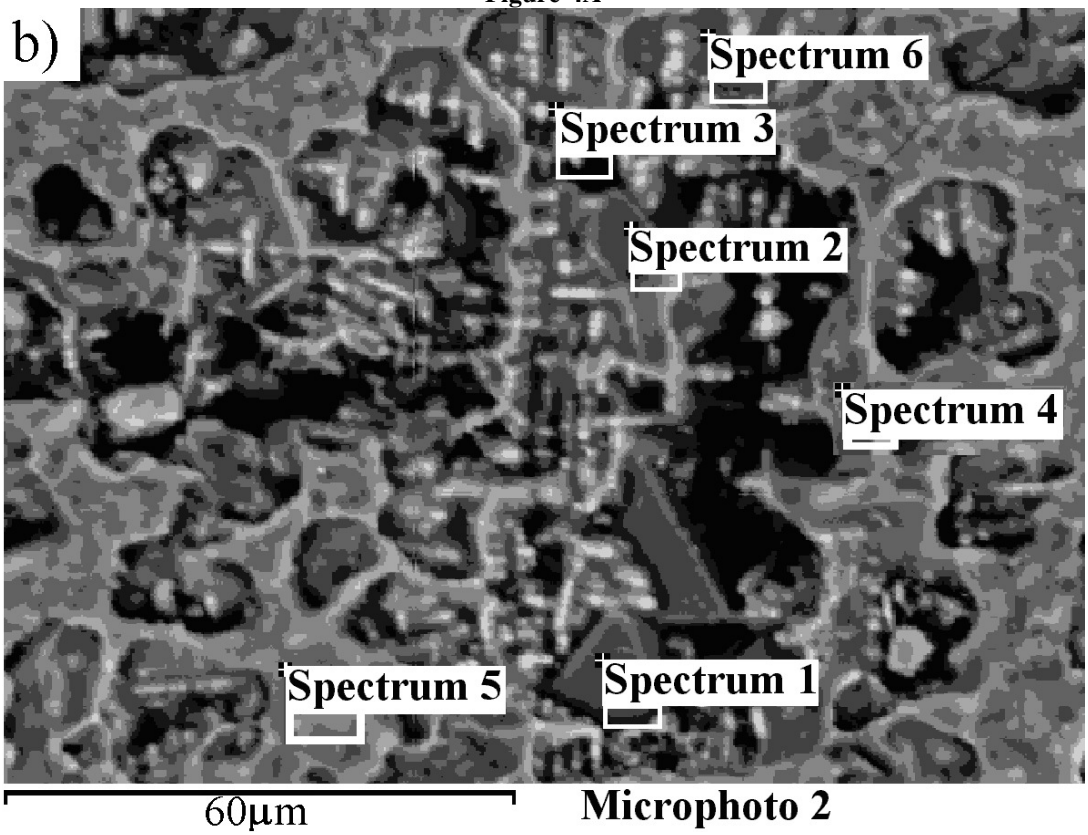

Figure-4B

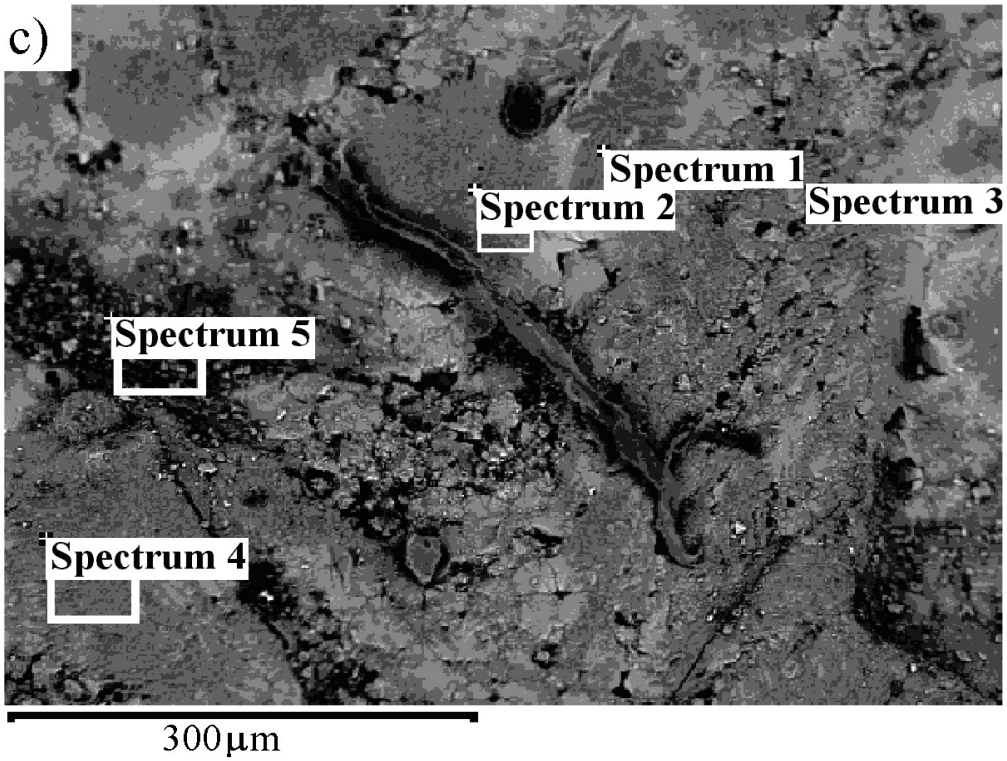

Figure-4C

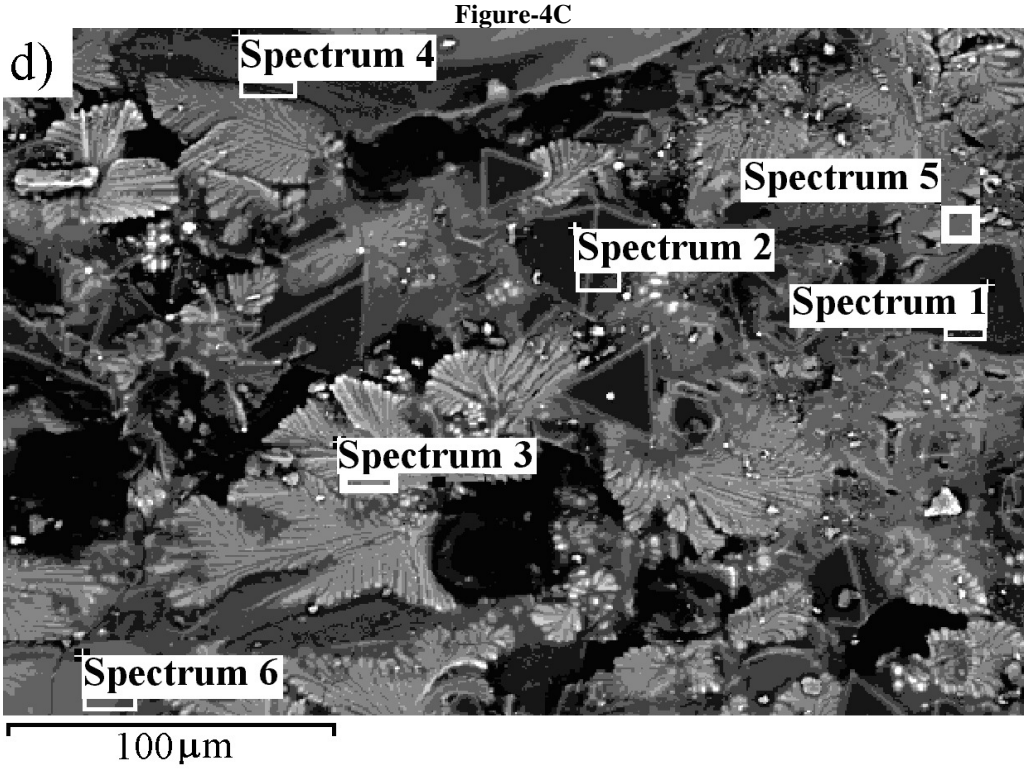

Figure-4D
Figure-4

SEM microphotos of the slag samples taken from the inner (a, b) and the upper (c, d) parts of the crucible and the region of EDX microanalysis. EDX spectra: a) 2, 4 – Mg_2SiO_4; b) 1, 2 – $MgAl_2O_4$, 3 – CaF_2; c)2 – $Ca_xMg_{2-x}SiO_4$ (x = 0.33), 3 – CaF_2; d) 1, 2 – $MgAl_2O_4$, 3 – CaF_2, 4 – Mg_2SiO_4. EDX spectra: a) 1, 3; b) 4–6; c) 1, 4, 5; d) 5, 6 correspond to amorphous-like phases with variable composition

Conclusion

HTXRD, XRPD and SEM/EDX studies were performed in order to obtain qualitative information on the products of high temperature treatment of the ceramic flux. The HTXRD study indicates a complex nature of the interaction in the ceramic flux, which is obtained utilizing liquid glass as a binder, before formation of the slag. The liquid phase forms simultaneously with the spinel $MgAl_2O_4$ phase that crystallized at ~1473 K. The slag obtained by the flux remelting at 1773 K according to XRPD data contains three phases: $MgAl_2O_4$, CaF_2 and Mg_2SiO_4. The latter phase and the solid solutions on its base ($Ca_xMg_{2-x}SiO_4$) are formed due to the interaction of CaF_2 with MgO and SiO_2. The SEM/EDX and HTXRD data indicate the non-uniform distribution of $MgAl_2O_4$ phase through the slag that potentially can result in a good slag separation from the surfaced metal.

References

1. Yu D.W. and Devletian J.H., Electroslag Surfacing: A potential process for rebuilding and restoration of ship components, Proc. of the NSRP 1988 Ship Production Symp., The society of naval architects and marine engineers (U.S.), Jersey City, 11A-1-18 **(1988)**

2. Kuskov Yu.M., Penetration of the parent metal in electroslag surfacing in a current-supplying solidification mould, *Weld. Int*., **16,** 48-50 **(2002)**

3. Cary H.B. and Helzer S.C., Modern Welding Technology, Pearson/Prentice-Hall, Upper Saddle River, 6th Ed., 736 **(2005)**

4. Podgaetskii V. and Lyuborets I., Welding fluxes, Naukova Dumka, Kiev, 165 **(1978)**

5. Podgaetskii V. and Kuzmenko V., Welding Slags. A Handbook, Naukova Dumka, Kiev, 253 **(1988)**

6. Wright S., Zhang L., Sun S. and Jahanshahi S., Viscosity of a CaO-MgO-Al_2O_3-SiO_2 melt containing spinel particles at 1646 K, *Metall. Mater. Trans. B*, **31**, 97-104 **(2000)**

7. Nightingale S.A. and Monaghan B.J., Kinetics of spinel formation and growth during dissolution of MgO in CaO-Al_2O_3-SiO_2 slag, *Metall. Mater. Trans.* B, **39**, 644-648 **(2008)**

8. Park J.H., The effect of boron oxide on the crystallization behavior of $MgAl_2O_4$ spinel phase during the cooling of the CaO-SiO_2-10 mass.% MgO-30 mass.%Al_2O_3 systems, *Met. Mater. Int.*, **16,** 987-992 **(2010)**

9. Park J.H., Solidification behavior of calcium aluminosilicate melts containing magnesia and fluorspar, *J. Am. Ceram. Soc*., **89,** 608-615 **(2006)**

10. Park J.H., Solidification structure of CaO–SiO_2–MgO–Al_2O_3(–CaF_2) systems and computational phase equilibria: Crystallization of $MgAl_2O_4$ spinel, *CALPHAD*, **31**, 428-437 **(2007)**

11. Sokolsky V.E., Roik A.S., Davidenko A.O., Kazimirov V.P., Lisnyak V.V., Galinich V.I. and Goncharov I.A., X-Ray diffraction and SEM/EDX studies on technological evolution of the oxide-fluoride ceramic flux for submerged arc-surfacing, *J. Min. Metall. Sect. B Metall.*, **48**, 101-113 **(2012)**

12. Kraus W. and Nolze G. Powder cell 3.2, Federal Institute for Materials Research and Testing (BAM), available online at: http://www.ccp14.ac.uk/ccp/web-mirrors/powdcell/a_v/v_1/powder/e_cell.html, (10.01.2012) **(2012)**

13. Match! Phase Identification from Powder Diffraction, Crystal Impact, available online at http://www.crystalimpact.com/match/download.htm, (10.01.2012) **(2012)**

14. Sokol'skii V.E., Kazimirov V.P. and Kuzmenko V.G., X-ray diffraction study of the multi component oxide systems, *J. Molec. Liq*., **93**, 235-238 **(2001)**

15. Rooi Ping L., Azad A.-M. and Wan Dung T., Magnesium aluminate ($MgAl_2O_4$) spinel produced via self-heat-sustained (SHS) technique, *Mat. Res. Bull*., **36**, 1417-1430 **(2001)**